JOURNAL OF AGRICULTURAL AND FOOD CHEMISTRY

ARTICLES

Analysis of Regiospecific Triacylglycerols by Electrospray Ionization−Mass Spectrometry^3 of Lithiated Adducts

JIANN-TSYH LIN* AND ARTHUR ARCINAS

Western Regional Research Center, Agricultural Research Service, U.S. Department of Agriculture, 800 Buchanan Street, Albany, California 94710

A method of regiospecific analysis of triacylglycerols (TAGs) in vegetable oils and animal fats is reported here using the electrospray ionization−mass spectrometry (MS^3) of TAG-lithiated adducts. The fragment ions of the MS^3 from the loss of fatty acids at the *sn*-2 position as α,β-unsaturated fatty acids were used for regiospecific identification and quantification. The ratio of the regiospecific TAGs, ABA and AAB, in an oil sample usually fraction collected by high-performance liquid chromatography can be determined by the abundance of the fragment ions of $[ABA + Li - \underline{A}COOH - \underline{B}'CH{=}CHCOOH]^+$ and $[AAB + Li - \underline{A}COOH - \underline{A}'CH{=}CHCOOH]^+$. The method was used to analyze regiospecific TAGs in extra virgin olive oil. The results showed that the saturated fatty acids, palmitic and stearic acids, were mostly located at the *sn*-1,3 positions and unsaturated fatty acids, oleic and linoleic acids, were mostly located at the *sn*-2 position.

KEYWORDS: Regiospecific; triacylglycerols; electrospray ionization; mass spectrometry; lithiated adducts; α,β-unsaturated fatty acids; olive oil

INTRODUCTION

Stereospecific (*sn*-1, *sn*-2, and *sn*-3, **Figure 1**) and regiospecific (*sn*-2 and *sn*-1,3) identification of acyl chains in the molecules of triacylglycerols (TAGs) from biological origins can be used in determining the acylation steps in the biosynthetic pathway of TAGs. The understanding of the biosynthesis is important in developing a transgenic oil seed plant that produces seed oil containing the desired fatty acid (FA) and acylglycerol (AG) components. Regiospecific locations of acyl chains affect the physical properties of the oils for industrial uses, for example, viscosity, pour point, melting point, heat of fusion, solubility, crystal structure, and polymorphism (*1*). It also affects the human absorption of TAGs in food and is thus valuable in nutritional value for the food industry. Currently, mass spectrometry (MS) cannot differentiate the stereoisomers of *sn*-1 and *sn*-3 of TAGs.

Regioisomers of TAGs in biological samples have been identified by atmospheric pressure chemical ionization−MS (APCI-MS) (*2, 3*) and by electrospray ionization−MS (ESI-MS) (*4, 5*) based on the premise that the loss of the acyl chain from the *sn*-1 or *sn*-3 position is energetically favored over the loss from the *sn*-2 position (**Figure 1**). The quantification of the regioisomers, dilinoleoyloleoylglycerol (LOL and LLO), has been determined from a linear calibration curve of the ratio of $[LL]^+$ and $[LO]^+$ fragment ions derived from various concentrations of regiospecific LOL and LLO standards by APCI-MS (*6, 7*). Recently, calibration curves of LLO, LOO, POO, and PPO using different mass spectrometric and liquid chromatographic methods were used for the quantification of oils and fat (*8*).

The regiospecific characterization of TAGs as lithiated adducts by collisionally activated dissociation tandem MS (CAD-MS^2) has been reported by Hsu and Turk (*9*). The ions reported from the loss of FAs as α,β-unsaturated FA specific at the *sn*-2 position of TAGs of lithiated adducts can be used for the regiospecific identification. We have recently identified and quantified six regiospecific diricinoleoylacylglycerols (RRAc) containing ricinoleate (a hydroxyl FA) in castor oil (*10*) using these ions. A method using ESI-MS^3 of lithiated TAGs to identify and quantify the regiospecific TAGs containing only common FAs (nonhydroxyl FAs) is reported here. The method used for the regiospecific TAGs, ABA and AAB, containing only common FAs described here is more complicated than that of RRAc (*10*), because AAB can also produce the ion from the loss of a common FA, B, specific at *sn*-1,3 positions as α,β-unsaturated FA in the ESI-MS^3 of lithiated TAGs. We have used this method to quantify the regiospecific ABA and AAB in extra virgin olive oil. The method can also be used to quantify regiospecific ABA and AAB in other vegetable oils and animal fats. The current MS^3 method can target the specific

* To whom correspondence should be addressed. Tel: 510-559-5764. Fax: 510-559-5768. E-mail: jiann.lin@ars.usda.gov.

10.1021/jf072837k
Published on Web 06/13/2008

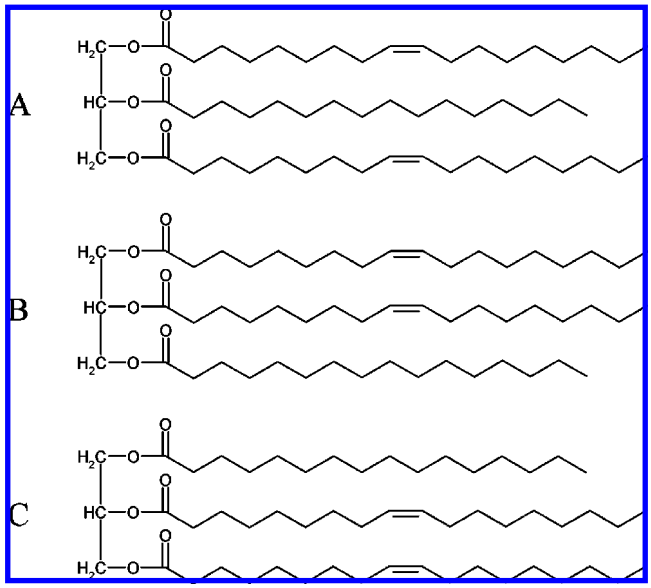

Figure 1. Structures of stereospecific dioleoylpalmitoylglycerols. (**A**) 1,3-Dioleoyl-2-palmitoyl-*sn*-glycerol, (**B**) 1,2-dioleoyl-3-palmitoyl-*sn*-glycerol, and (**C**) 2,3-dioleoyl-1-palmitoyl-*sn*-glycerol.

molecular species of ABA and AAB in a biological sample and can thus avoid the contamination of ions from other molecular species (*6*).

EXPERIMENTAL PROCEDURES

Materials. TAG standards and lithium acetate were obtained from Sigma (St. Louis, MO). High-performance liquid chromatography (HPLC) and gas chromatography grade methanol and 2-propanol (Burdick & Jackson) for liquid chromatography−mass spectrometry (LC-MS) were purchased from Fisher Scientific (Pittsburgh, PA). High-purity nitrogen for LC-MS was acquired from Praxair (Oakland, CA). Research grade (99.999%) helium (Praxair) was used as a collision gas. Extra virgin olive oil (Lucini, Italia, first cold press) was purchased from a local store.

HPLC Fractionation of the Molecular Species of TAGs in Olive Oil. The fractionation of the molecular species of TAGs in olive oil was prepared as previously reported (*11*). Chromatographic fractionation was performed using a Waters HPLC (Waters Associate, Milford, MA) and a C_{18} analytical column (Gemini, 250 mm × 4.6 mm, 5 μm, C18, Phenomenex, Torrance, CA). One milligram of olive oil was chromatographed at 22 °C (room temperature) with a linear gradient from 100% methanol to 100% 2-propanol in 40 min, at a 1 mL/min flow rate, and detected at 205 nm. One-half minute fractions were collected, and analogous fractions were pooled from eight HPLC runs. Four major HPLC peaks were collected at fractions 62−64 (containing LLO and LLP), fractions 65−68 (containing OOL, POL, and PPL), fractions 69−71 (containing OOO, OOP, and PPO), and fractions 72−74 (containing OOS and POS), TAGs with the same partition numbers together. The four combined fractions collected were evaporated to dryness. The final sample solutions prepared for direct infusion (200 μL) into the MS were the mixtures of 100 μL of dichloromethane solution containing 100 μg of the targeted molecular species, 100 μL of methanol, and 50 μL of methanol solution of lithium acetate (100 mM). TAG concentrations were roughly estimated from previously published olive oil data (*12*).

ESI-MS^3 of TAG. An LCQ Advantage quadrupole ion-trap mass spectrometer with Xcalibur 1.3 software (ThermoFinnigan, San Jose, CA) was utilized for MS analysis of the various TAGs. Direct infusion of 200 μL samples was from the mixture of 100 μL of dichloromethane solution containing about 25 μg TAG standards, 100 μL of methanol, and 50 μL of methanol solution of lithium acetate (100 mM). The infusion at a 2.5 μL/min flow rate from a syringe pump produced stable singly charged lithiated parent ions, which were subsequently fragmented for MS^2 and MS^3 analysis. ESI source conditions were as follows: 50 arbitrary units (au) nitrogen sheath gas flow rate, 4.5 kV spray voltage, 250 °C ion-transfer capillary temperature, 1.5 *m/z* isolation width, 160−1000 *m/z* mass range, 5 min acquisition time, 38 V capillary voltage, and normalized collision energy ranging 35−46% for both MS^2 and MS^3 fragmentations, varying between molecular species of TAGs.

RESULTS AND DISCUSSION

The regiospecific analysis of TAGs, *sn*-ABA and *sn*-AAB, containing only common FAs (nonhydroxyl FAs), is described here by ESI-MS^3 of lithiated adducts. **Figure 1** shows the structures of *sn*-OPO (1,3-dioleoyl-2-palmitoyl-*sn*-glycerol), *sn*-OOP (1,2-dioleoyl-3-palmitoyl-*sn*-glycerol), and *sn*-POO (1-palmitoyl-2,3-dioleoyl-*sn*-glycerol). Currently, *sn*-AAB and *sn*-BAA are not commercially available and cannot be differentiated by MS. AAB shown here is the mixture of AAB and BAA as 1(3),2-dioleoyl-3(1)-palmitoyl-*sn*-glycerol unless specified. ABA shown here is stereospecific as *sn*-ABA.

Figure 2 shows the MS^2 spectrum of $[OPO + Li]^+$ at *m/z* 865.5. The spectrum is simple and shows the precursor ion and the fragment ions of $[OPO + Li - \underline{O}COOH]^+$ at *m/z* 583.4 and $[OPO + Li - \underline{P}COOH]^+$ at *m/z* 609.4, reflecting the neutral loss of oleic acid (OCOOH) and palmitic acid (PCOOH), respectively. The neutral loss of the lithium salts of these FAs was also observed at a lower abundance as $[OPO + Li - \underline{O}COOLi]^+$ at *m/z* 577.4 and $[OPO + Li - \underline{P}COOLi]^+$ at *m/z* 603.4 (*9*).

Figure 3 shows the MS^3 spectrum of $[OPO + Li - \underline{O}COOH]^+$ at *m/z* 583.5. A regiospecific ion was derived from the loss of palmitate specific at the *sn*-2 position as α,β-unsaturated palmitate corresponding to the ion of $[OPO + Li - \underline{O}COOH - \underline{P}'CH{=}CHCOOH]^+$ at *m/z* 329.2. The ion of $[OPO + Li - \underline{O}COOH - \underline{O}'CH{=}CHCOOH]^+$ at *m/z* 303 was not detected because oleoyl chain was not at the *sn*-2 position. The fragmentation pathway for the ions from the loss of FAs specific at the *sn*-2 position as α,β-unsaturated FAs from TAG lithiated adducts was previously proposed (*9*). An ion at *m/z* 527.3 (**Figure 3**) may be the acid anhydride of oleate and palmitate, $[\underline{O}COOCOP + Li]^+$, and is the same as $[OPO + Li - \underline{O}COOH - C_3H_4O]^+$. The loss of C_3H_4O was from the glycerol backbone. The fragmentation pathway for the formation of acid anhydride ion was proposed recently (*10*). Both postulated pathways involved the intermediate containing a 1,3-dioxolane five-membered ring with the two carbon atoms of the ring originating from the glycerol backbone. **Figure 3** also shows oleate, $[\underline{O}COOH + Li]^+$ at *m/z* 289.2, and to lesser extent palmitate, $[\underline{P}COOH + Li]^+$ at *m/z* 263.2.

Figure 3 also shows the minor ions from the loss of ketenes as $[OPO + Li - \underline{O}COOH - \underline{O}''CH{=}C{=}O]^+$ at *m/z* 319.2 and $[OPO + Li - \underline{O}COOH - \underline{P}''CH{=}C{=}O]^+$ at *m/z* 345.2. The abundance of the ion at *m/z* 319.2 was about twice that of the ion at *m/z* 345.2, indicating that the loss of ketene at the *sn*-1,3 position was in favor to that of the *sn*-2 position for the TAG. The ions from the loss of ketenes as lithiated adducts and the proposed fragmentation pathway have been reported (*9*).

Figure 4 shows the MS^3 spectrum of $[OPO + Li - \underline{P}COOH]^+$ at *m/z* 609.3. The major fragment ion $[OPO + Li - \underline{P}COOH - \underline{O}'CH{=}CHCOOH]^+$ at *m/z* 329.2 was apparently from the loss of FA at the *sn*-1(3) position as α,β-unsaturated oleate, because the precursor ion contained no oleoyl chain at the *sn*-2 position. As shown in **Figure 3**, the precursor ion containing an acyl chain at the *sn*-2 position produced a fragment ion from the loss of a FA as α,β-unsaturated FA at the *sn*-2 position only, not *sn*-1,3 positions. As shown in **Figure 4**, the precursor ion containing no acyl chain at the *sn*-2 position produced a fragment ion from the loss of a FA as α,β-unsaturated acyl chain at the *sn*-1,3 position.

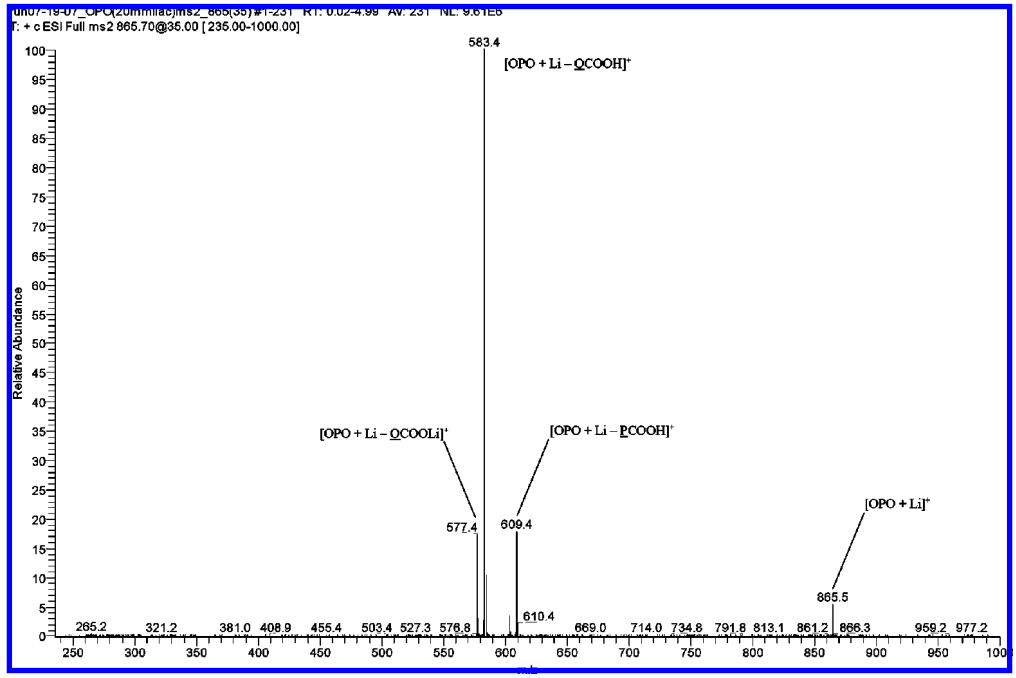

Figure 2. Ion trap mass spectrum of ESI-MS^2 of $[OPO + Li]^+$ ion at *m/z* 865.5. Abbreviations: Both O and OCOOH are oleic acid. Both P and PCOOH are palmitic acid. OPO is 1,3-dioleoy-2-palmitoyl-*sn*-glycerol. OCOOLi is the lithium salt of oleic acid.

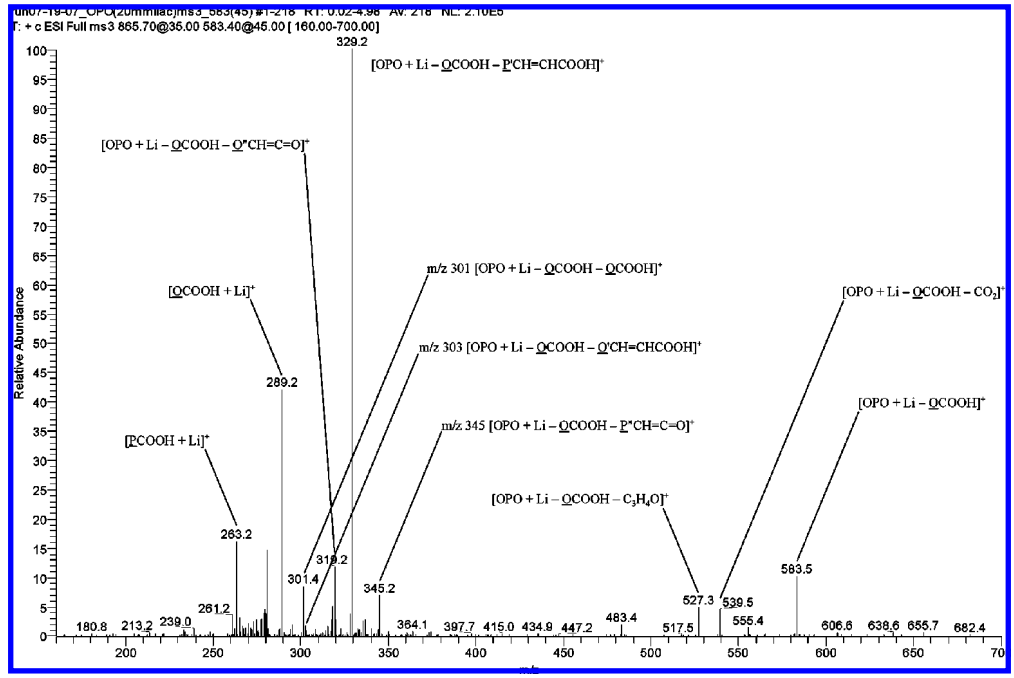

Figure 3. Ion trap mass spectrum of ESI-MS^3 of $[OPO + Li - OCOOH]^+$ at *m/z* 583.5. For abbreviations, see **Figure 2**. P′CH═CHCOOH is the α,β-unsaturated palmitic acid from the *sn*-2 position. O′CH═CHCOOH is α,β-unsaturated oleic acid from the *sn*-1,3 position (not detected). C_3H_4O is the loss of glycerol backbone to form acid anhydride of two FAs (*6*). P″CH═C═O is palmitoyl ketene from the *sn*-2 position, and O″CH═C═O is oleoyl ketene from the *sn*-1,3 position.

The MS^3 spectrum of $[OOP + Li - PCOOH]^+$ at *m/z* 609.3 (unpublished) was very much similar to that of $[OPO + Li - PCOOH]^+$ at *m/z* 609.3 (**Figure 4**), including the precursor ion and significant fragment ions and their relative abundance. The MS^3 spectra of other ABA, POP, OSO, and SOS were similar to those of **Figures 3** and **4**: $[ABA + Li - ACOOH - B'CH{=}CHCOOH]^+$ were detected, and $[ABA + Li - ACOOH - A'CH{=}CHCOOH]^+$ were not detected.

Figure 5 shows the MS^3 spectrum of $[OOP + Li - OCOOH]^+$ at *m/z* 583.4. This precursor ion was the mixture of 1,2-PO and 1,3-OP from OOP. The precursor ion, 1,3-OP, produced the fragment ions of both $[OOP + Li - OCOOH - P'CH{=}CHCOOH]^+$ at *m/z* 329 and $[OOP + Li - OCOOH - O'CH{=}CHCOOH]^+$ at *m/z* 303.1. The precursor ion, 1,2-PO, produced the fragment ion of $[OOP + Li - OCOOH - O'CH{=}CHCOOH]^+$ at *m/z* 303.1, but not $[OOP + Li - OCOOH - P'CH{=}CHCOOH]^+$ at *m/z* 329. The ratio of the abundance of these two fragment ions, *m/z* 329 and *m/z* 303.1, was 0.25. The fragment ion of $[OOP + Li - OCOOH - O'CH{=}CHCOOH]^+$ at *m/z* 303.1 was the base peak, while $[OOP + Li - OCOOH - P'CH{=}CHCOOH]^+$ at *m/z* 329 was a minor peak (25%). For the accurate quantification of the percentages of the regioisomers in

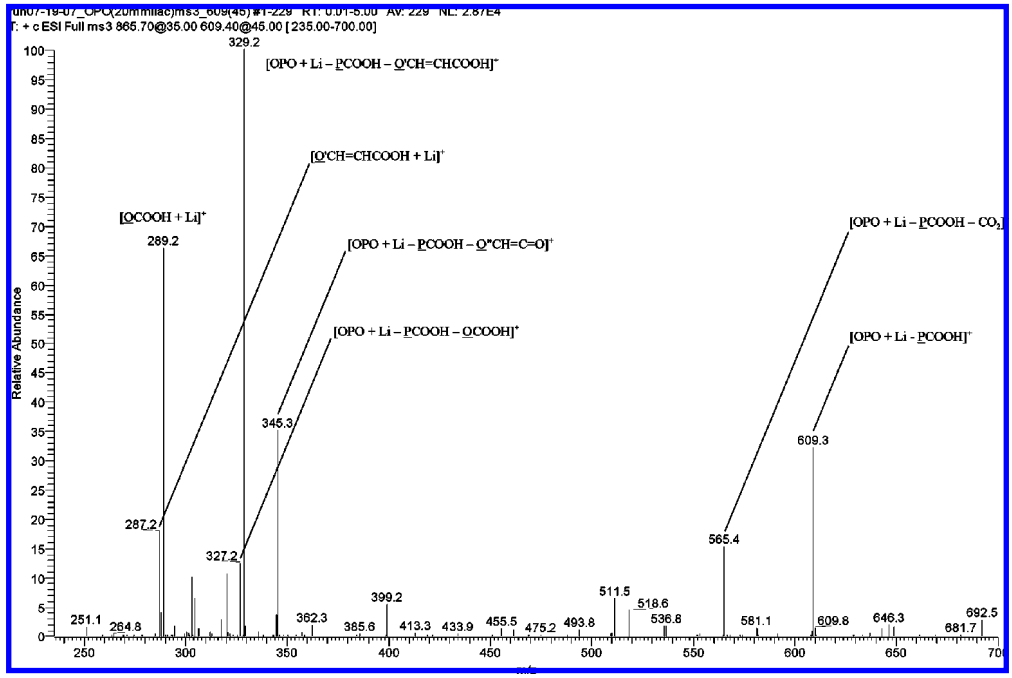

Figure 4. Ion trap mass spectrum of ESI-MS^3 of [OPO + Li − PCOOH]$^+$ at *m/z* 609.3. For abbreviations, see **Figures 2** and **3**. This spectrum is very much the same as that of ESI-MS^3 of [OOP + Li − PCOOH]$^+$ at *m/z* 609.3. OOP is the standard 1,2-dioleoy-3-palmitoyl-*rac*-glycerol.

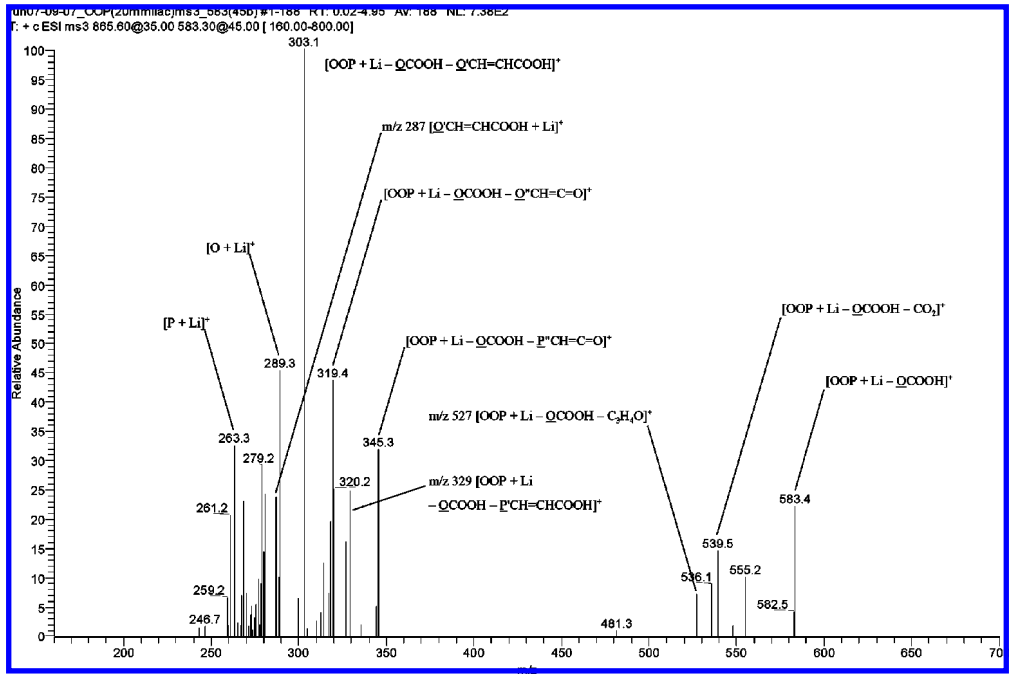

Figure 5. Ion trap mass spectrum of ESI-MS^3 of [OOP + Li − QCOOH]$^+$ at *m/z* 583.4. For abbreviations, see **Figures 2–4**.

the mixture of OPO and OOP, this minor peak from OOP must be considered, because it interferes with the ion [OPO + Li − QCOOH − P′CH=CHCOOH]$^+$ at *m/z* 329.2 from OPO.

Analysis of regiospecific OPO and OOP depends on the fragment ions from the loss of FA as α,*β*-unsaturated FAs specific at the *sn*-2 position. **Figure 3** from the OPO standard shows the major ion of [OPO + Li − QCOOH − P′CH=CHCOOH]$^+$ at *m/z* 329.2 from the loss of P′CH=CHCOOH at the *sn*-2 position, and the ion of [OOP + Li − QCOOH − O′CH=CHCOOH]$^+$ at *m/z* 303 was not detected. **Figure 5** from the regiospecific OOP standard shows the ion of [OOP + Li − QCOOH − O′CH=CHCOOH]$^+$ at *m/z* 303.1 at the *sn*-2 position and at less abundant the ion of [OOP + Li − QCOOH − P′CH=CHCOOH]$^+$ at *m/z* 329 from the loss of P′CH=CHCOOH at the *sn*-1,3 position. The ion at *m/z* 303.1 from the loss of O′CH=CHCOOH at the *sn*-2 position can be used to detect a very small amount of OOP because OPO does not produce the ion at *m/z* 303 (**Figure 3**).

The MS^3 spectrum of the sample containing both regiospecific OPO and OOP will be the mix of ions shown in **Figures 3** and **5**. The ratio of these two regioisomers can be estimated from the ratio of the abundance of the ions at *m/z* 329.2 and *m/z* 303.1 from the loss of FAs mostly at the *sn*-2 position as the α,*β*-unsaturated FAs in assuming a linear relationship (*6*). However, the ion observed at *m/z* 329.2 resulted not only from the loss of P′CH=CHCOOH at the *sn*-2 position of OPO but also from the loss of P′CH=CHCOOH at the *sn*-1,3 position of OOP to a lesser extent. The assumption was that the abundance of the ions [OOP + Li − QCOOH − O′CH=CHCOOH]$^+$ at *m/z* 303.1 and [OOP + Li −

Table 1. Ratios of the Peak Abundance of [AAB + Li − ACOOH − B′CH=CHCOOH]$^+$ and [AAB + Li − ACOOH − A′CH=CHCOOH]$^+$ on the MS^3 of TAG Standards, AAB, and Lithium Adducts[a]

AAB[b]	AAB + Li	AAB + Li − ACOOH	CE[c] of MS^2 (%)	CE[c] of MS^3 (%)	peak mass[d]	ratio
OOP	865.5	583.4	35	45	329/303	0.25
PPO	839.5	583.4	35	45	303/329	0.05
OOS	893.5	611.5	36	44	329/331	0.17
SSO	895.6	611.5	35	42	331/329	0.15
OOL	889.6	607.4	35	44	329/327	0.10
LLO	887.7	607.4	35	45	327/329	0.28
LLP	861.5	581.4	36	46	327/303	0.37
SSP	869.8	585.5	35	45	331/303	0.17

[a] Abbreviations: A, ACOOH and B are FAs, B′CH=CHCOOH is α,β-unsaturated FA from TAG AAB. [b] Abbreviations of TAGs: O, oleic acid; P, palmitic acid; S, stearic acid; and L, linoleic acid. [c] Collision energy. [d] The masses are [AAB + Li − ACOOH − B′CH=CHCOOH]$^+$/[AAB + Li − ACOOH − A′CH=CHCOOH]$^+$.

OCOOH − P′CH=CHCOOH]$^+$ at *m/z* 329 from OOP combined and the abundance of the ion [OPO + Li − OCOOH − P′CH=CHCOOH]$^+$ at *m/z* 329.2 from OPO were proportional to the ratio of OOP to OPO. The abundance of the ion [OOP + Li − OCOOH − P′CH=CHCOOH]$^+$ at *m/z* 329 from OOP in a sample of regiomixture can be estimated from the abundance of the ion at *m/z* 303 multiplied by the ratio of the abundance of *m/z* 329 and *m/z* 303 from the regiospecically pure OOP standard as shown in **Figure 5** and **Table 1**, which was determined to be 0.25. The MS^3 spectra of other AAB shown in **Table 1** also contained the ions of [AAB + Li − ACOOH − B′CH=CHCOOH]$^+$ and [AAB + Li − ACOOH − A′CH=CHCOOH]$^+$ as **Figure 5**.

Table 1 shows the ratios of the ion abundance of [AAB + Li − ACOOH − B′CH=CHCOOH]$^+$ and [AAB + Li − ACOOH − A′CH=CHCOOH]$^+$ from the MS^3 fragmentation of various commercially available TAG standards, AAB. The ratio varied depending upon the molecular species of AAB and MS operating conditions, including the collision energies of MS^2 and MS^3 fragmentations. The collision energies used to obtain MS^3 spectra from commercially available standards are given in **Table 1**. In the analysis of biological samples, the MS operating conditions should be the same as those of the AAB standards. Lower ratio values of ion abundance from [AAB + Li − ACOOH − B′CH=CHCOOH]$^+$ and [AAB + Li − ACOOH − A′CH=CHCOOH]$^+$ can provide a more accurate ratio of the regioisomers, because of less contribution from the abundance of [AAB + Li − ACOOH − B′CH=CHCOOH]$^+$ toward the same *m/z* value from [ABA + Li − ACOOH − B′CH=CHCOOH]$^+$. The data in **Table 1** have been shown to be reproducible.

In the MS^3 analysis of TAGs containing only nonhydroxyl acyl chains, the fragment ions from the loss of acyl chains as α,β-unsaturated FAs mostly from the *sn*-2 position were major ions as shown in **Figures 3–5**. The MS^3 fragmentation of RAcR and RRAc (*10*) showed that the loss of acyl chains as α,β-unsaturated FAs were minor ions and from the *sn*-2 position only. These ions were less abundant than the fragment ions from the loss of two FAs, [RAcR + Li − COOH − AcCOOH]$^+$ (*10*). In the MS^3 analysis of TAGs containing only nonhydroxyl FAs, the fragment ions from the loss of two FAs were either not detected or were very minor ions, such as [OPO + Li − OCOOH − PCOOH]$^+$ at *m/z* 327 in **Figure 3**, [OPO + Li − PCOOH − OCOOH]$^+$ at *m/z* 327.2 in **Figure 4**, and [OOP + Li − OCOOH − OCOOH]$^+$ at *m/z* 301 in **Figure 5**.

Identification and quantification of the molecular species of TAGs (nonregiospecific) in olive oil by MS have been recently reported (*12–14*). The contents varied, and the latest report (*12*) showed that the TAG (nonregiospecific) contents in olive oil (Aix-en-Provence, France) were as follows: OOO (35%), OOP (22%,), OOL (15%), PLO (7.7%), PPO (3.6%), OOS (3.2%), LLO (2.9%), LLP (1.1%), and PPL (0.8%). The quantitative regiospecific analysis of AAB and ABA in olive oil has only been reported for regiospecific LOL as 0% among LLO, LOL, and OLL combined (*6*). The presence of some regiospecific OOP, OOS, OLO, LLO, POP, and LLP in olive oil has also been reported (*2*).

Figure 6 shows the ion trap mass spectrum of ESI-MS^3 of [OOP + Li − OCOOH]$^+$ and [OPO + Li − OCOOH]$^+$ at *m/z* 583.6 from the HPLC fraction of olive oil containing OOO, OOP (OPO) and PPO (POP) (same partition numbers). The ratio of the abundance of *m/z* 329.3 and 303.2 was 31% from the mixture of OOP and OPO in olive oil (**Figure 6**). The ion *m/z* 303.2 resulted from [OOP + Li − OCOOH − O′CH=CHCOOH]$^+$ alone, while the ion *m/z* 329.3 originated from both [OOP + Li − OCOOH − P′CH=CHCOOH]$^+$ and [OPO + Li − OCOOH − P′CH=CHCOOH]$^+$. According to the ratio of OOP in **Table 1** as 25%, the abundance of ions [OOP + Li − OCOOH − O′CH=CHCOOH]$^+$ at *m/z* 303.2 and [OOP + Li − OCOOH − P′CH=CHCOOH]$^+$ at *m/z* 329.3 from OOP combined was 100 + 25 = 125%. The abundance of these three ions combined was 100 + 31 = 131%. The content of OOP (and POO) among the three stereoisomers (OOP, OPO, and POO) combined was 125 divided by 131 or 95%.

Again, in the biological sample containing a mixture of ABA and AAB, the *m/z* value, the same as [AAB + Li − ACOOH − A′CH=CHCOOH]$^+$, was provided from AAB alone without contribution from the [ABA + Li − ACOOH − A′CH=CHCOOH]$^+$ ion (**Figure 3**). A minor amount of AAB can be detected by this method because ABA could not contribute to this ion. The mixture of AAB and ABA produced the ions of [AAB + Li − ACOOH − B′CH=CHCOOH]$^+$ and [ABA + Li − ACOOH − B′CH=CHCOOH]$^+$ at the same *m/z* value (**Figure 6**, *m/z* 329.3). The abundance of [AAB + Li − ACOOH − B′CH=CHCOOH]$^+$ may be determined from the abundance of [AAB + Li − ACOOH − A′CH=CHCOOH]$^+$ multiplied by the ratio in **Table 1**. The relative abundance of the ions of [AAB + Li − ACOOH − A′CH=CHCOOH] and [AAB + Li − ACOOH − B′CH=CHCOOH]$^+$ from AAB combined and the ion [ABA + Li − ACOOH − B′CH=CHCOOH]$^+$ from ABA were used proportionally (assuming a linear relationship) to estimate the content of AAB and ABA.

We have used the current method to estimate approximately the contents of regioisomers of ABA and AAB in the three stereoisomers (AAB, ABA, and BAA) combined in olive oil as follows: OOP (95%), POP (98%), OOL (61%), OOS (94%), PLP (100%), LLO (67%), and LLP (74%). AAB also includes BAA. For the quantification of PLP by the current MS^3 method, there was no PPL standard available for the ratio (**Table 1**). The ion, [PLP + Li − PCOOH − L′CH=CHCOOH]$^+$ at *m/z* 303, was the base peak, and the ion, [PPL + Li − PCOOH − P′CH=CHCOOH]$^+$ at *m/z* 327, was not detected. Therefore, the content of PLP was determined to be 100%. The saturated FAs, palmitic and stearic acids, were mostly located at the *sn*-1,3 positions, and the unsaturated FAs, oleic and linoleic acids, were mostly located at the *sn*-2 position. On the plant TAG biosynthetic pathway, unsaturated FAs are incorporated mostly at the *sn*-2 position.

By the earlier method (*6*), LLO in olive oil was estimated as about 100% and by the current method as 67%. The current method (MS^3) can differentiate the molecular species by masses, for example, LLO (LLO, OLL, and LOL) and LLP (LLP, PLL, and LPL). The earlier method of APCI/MS^1 might produce the

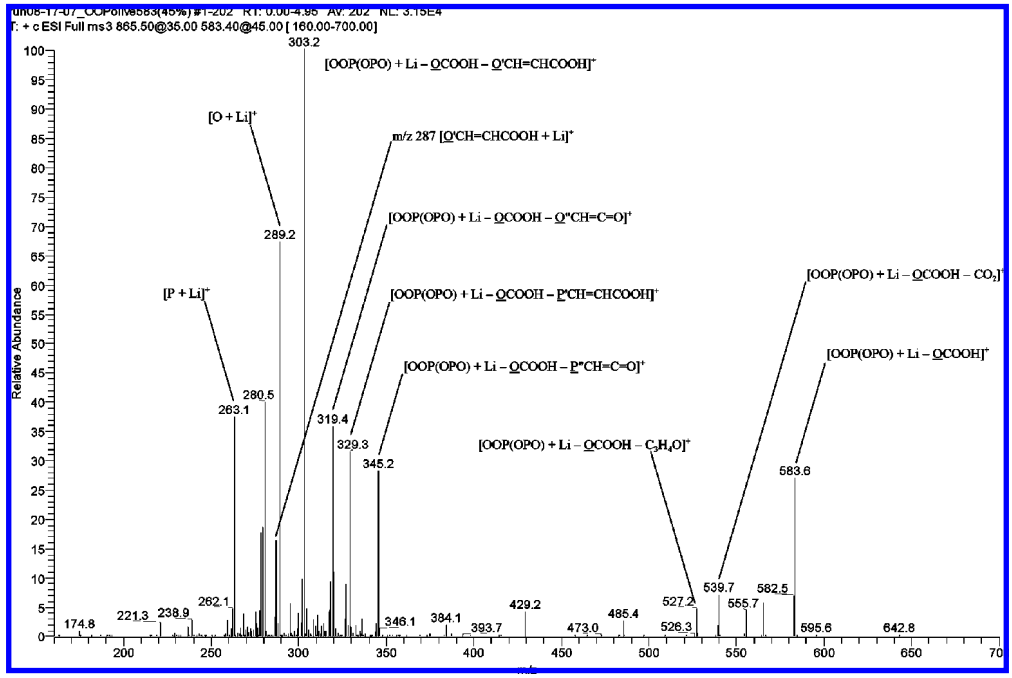

Figure 6. Ion trap mass spectrum of ESI-MS^3 of $[OOP(OPO) + Li - \underline{O}COOH]^+$ at *m/z* 583.6 from the HPLC fraction of olive oil containing OOO (triolein) as a major component in this fraction. For abbreviations, see **Figures 2–4**.

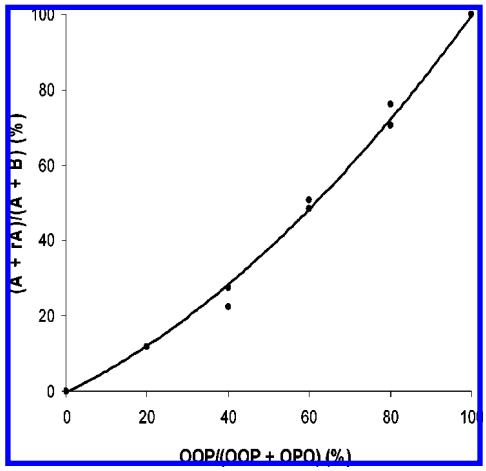

Figure 7. Calibration curve of the content of regioisomer (OOP) estimated at various contents of OOP in the mixture of OOP and OPO. *A* = the abundance of *m/z* at 303.1 from the mixture of OOP and OPO. *B* = the abundance of *m/z* at 329.2 from the mixture of OOP and OPO. *r* = the ratio of the abundance of *m/z* 329 and *m/z* 303.1 from OOP standard; see **Figure 5**. OOP = content of OOP, and OPO = content of OPO.

same DAG ions from two different molecular species, for example, $[LL]^+$ from LLO and LLP, which are difficult to separate by HPLC (*2, 6, 11*). TAGs with the same partition number are also difficult to separate by HPLC. The current ion trap MS^3 method with isolation width of 1.5 *m/z* at both MS^2 and MS^3 stages for the biological samples is much more specific to the targeted molecular species than the earlier MS^1 method. The current quantification method is suitable for the TAG in **Table 1** with 16 and 18 carbon atoms. The TAGs with FA residues of very different chain lengths or very different degree of unsaturation may be applicable but need to be proved. The regioisomers can be confirmed by the hydrolysis of TAGs using *sn*-1,3 specific lipase and the MS of the hydrolytes as we recently reported (*15*).

Calibration curves have been used for the quantification of regioisomers (*6, 8*). **Figure 7** shows the calibration curve, which was near linear, using different ratios of OOP and OPO. The reason that this was not a straight line might be because this was an MS^3 (two fragmentations) study. The current method is applicable for quantification; however, using calibration curves from each regioisomeric pairs could be more accurate but more time-consuming. Using the calibration curve of **Figure 7** for estimation, the OOP content among OOP and OPO combined in olive oil would be 97%, which is reasonably close to the 95% estimated by the current method. However, the region of greatest deviation (see **Figure 7**) gave a 40% estimate by the current method (linear relationship) as compared to 51% by the calibration curve (**Figure 7**). The ratios shown in **Table 1** could vary if MS conditions change; therefore, it is ideal to obtain the ratio values or calibration curves the same day or within a few days after TAG samples are analyzed.

LITERATURE CITED

(1) Foubert, I.; Dewettinck, K.; Van de Walle, D.; Dijkstra, A. J.; Quinn, P. J. Physical properties: Structural and physical characteristics. In *The Lipid Handbook*, 3rd ed.; Gunstone, F. D, Harwood, J. L. , Dijkstra, A. J., Eds.; CRC Press, Taylor & Francis Group: Boca Raton, FL, 2007; Chapter 8, pp 535−590.

(2) Mottram, H. R.; Woodbury, S. E.; Evershed, R. P. Identification of triacylglycerol positional isomers present in vegetable oils by high performance liquid chromatography/atmospheric pressure chemical ionization mass spectrometry. *Rapid Commun. Mass Spectrom.* **1997**, *11*, 1240–1252.

(3) Mottram, H. R.; Crossman, Z. M.; Evershed, R. P. Regiospecific characterization of the triacylglycerols in animal fats using high performance liquid chromatography-atmospheric pressure chemical ionization mass spectrometry. *Analyst* **2001**, *126*, 1018–1024.

(4) Kalo, P.; Kemppinen, A.; Ollilainen, V.; Kuksis, A. Regiospecific determination of short-chain triacylglycerols in butterfat by normal-phase HPLC with on-line electrospray-tandem mass spectrometry. *Lipids* **2004**, *39*, 915–928.

(5) Marzilli, L. A.; Fay, L. B.; Dionisi, F.; Vouros, P. Structural characterization of triacylglycerols using elctrospray ionization-MS^n ion-trap MS. *J. Am. Oil Chem. Soc.* **2003**, *80*, 195–202.

(6) Jakab, A.; Jablonkai, I.; Forgacs, E. Quantification of the ratio of positional isomer dilinoleoyl-oleoyl glycerols in vegetable oils. *Rapid Commun. Mass Spectrom.* **2003**, *17*, 2295–2302.
(7) Byrdwell, W. C. The bottom-up solution to the triacylglycerol lipidome using atmospheric pressure chemical ionization mass spectrometry. *Lipids* **2005**, *40*, 383–417.
(8) Leskinen, H.; Suomela, J. P.; Kallio, H. Quantification of triacylglycerol regioisomers in oils and fat using different mass spectrometric and liquid chromatographic methods. *Rapid Commun. Mass Spectrom.* **2007**, *21*, 2361–2373.
(9) Hsu, F.-F.; Turk, J. Structural characterization of triacylglycerols as lithiated adducts by electrospray ionization mass spectrometry using low-energy collisionally activated dissociation on a triple stage quadrupole instrument. *J. Am. Soc. Mass Spectrom.* **1999**, *10*, 587–599.
(10) Lin, J. T.; Arcinas, A. Regiospecific analysis of diricinoleoylacylglycerols in castor (*Ricinus communis* L.) oil by electrospray ionization-mass spectrometry. *J. Agric. Food Chem.* **2007**, *55*, 2209–2216.
(11) Lin, J. T.; Woodruff, C. L.; McKeon, T. A. Non-aqueous reversed-phase high-performance liquid chromatography of synthetic triacylglycerols and diacylglycerols. *J. Chromatogr. A* **1997**, *782*, 41–48.
(12) Ollivier, D.; Artaud, J.; Pinatel, C.; Durbec, J.; Guerere, M. Differentiation of French virgin oil RDOs by sensory characteristics, fatty acids and triacylglycerol compositions and chemometrics. *Food Chem.* **2006**, *97*, 382–393.
(13) Jakab, A.; Heberger, K.; Forgacs, E. Comparative analysis of different plant oils by high-performance liquid chromatography-atomospheric pressure chemical ionization mass spectrometry. *J. Chromatogr. A* **2002**, *976*, 255–263.
(14) Gomez-Ariza, J. L.; Arias-Borrego, A.; Garcia-Barrera, T.; Beltran, R. Comparative study of electrospray ionization sources coupled to quadrupole time-of-flight mass spectrometer forolive oil authentication. *Talanta* **2006**, *70*, 859–869.
(15) Lin, J. T.; Arcinas, A. Regiospecific identification of 2-(12-ricinoleoylricinoleoyl)-1,3-*sn*-diricinoleoyl-glycerol in castor (*Ricinus communis* L.) oil by ESI-MS4, *J. Agric. Food Chem.* **2008**, *56*, 3616–3622.

Received for review September 24, 2007. Revised manuscript received April 18, 2008. Accepted April 20, 2008.

JF072837K